

## In-vitro activity and tissue distribution of new fluorinated *meso*-tetrahydroxyphenylporphyrin photosensitizers

Sandile P. Songca

### Abstract

Tetra(hydroxyphenyl)porphyrins started to attract interest as potential photosensitizers for photodynamic therapy in the early eighties. Subsequently, a number of derivatives of these compounds have been studied. In 1997 we reported the synthesis of the fluorinated derivatives 5,10,15,20-tetrakis(2-fluoro-3-hydroxyphenyl)porphyrin (**8**), 5,10,15,20-tetrakis(2,4-difluoro-3-hydroxyphenyl)porphyrin (**9**), and 5,10,15,20-tetrakis(3,5-difluoro-4-hydroxyphenyl)porphyrin (**10**). We have measured their biological activity, using the MTT test, against cancer cell cultures in-vitro. The test showed that these compounds were as potent as 5,10,15,20-tetrakis(3-hydroxyphenyl)chlorin (**5**), one of the leading photosensitizers in photodynamic therapy. The highest photoactivity was shown by the *meta*-hydroxy compounds **8** and **9**. The *para*-compound showed high toxicity in the dark. Distribution of these compounds between normal and cancer tissue was studied using  $^{19}\text{F}$  NMR spectroscopy. The highest cancer tissue localization was also shown by the *meta*-hydroxy compounds **8** and **9**. The *para* compound showed poor localization in tumour tissue. This study has shown that  $^{19}\text{F}$  NMR spectroscopy can be used to estimate the tissue distribution of fluorinated tetrahydroxyphenylporphyrins in-vivo.

Chemistry Department,  
University of Transkei, Private  
Bag X1, Umtata, Umtata, 5100,  
Eastern Cape, South Africa  
Sandile P. Songca

**Correspondence:** S. P. Songca,  
Chemistry Department,  
University of Transkei, Private  
Bag X1, Umtata, Umtata, 5100,  
Eastern Cape, South Africa.

**Funding:** This work was supported by the University of Transkei (University Research Programme), the National Research Foundation (IRDP), Luthuli Memorial Trust, and by United Nations Education and Training Programme for Southern Africa. Generous grants from Sentrachem, Liberty Life Foundation and TWAS are greatly appreciated.

### Introduction

Photodynamic therapy is based on two important biological properties of photodynamic therapy drugs; their preferential tumour localization and their destruction of animal tissue in the presence of light and oxygen (McRobert et al 1989). In the principal cell destruction mechanism, these organic compounds, notably porphyrins and phthalocyanines, are believed to photosensitize normal triplet state oxygen, which is always present in significant amounts in tissues, to produce singlet oxygen, a powerful oxidant which is known to lead to cell destruction by a variety of pathways (Neely et al 1988). In a typical treatment of tumorous cancer with photodynamic therapy, the patient is injected intravenously with a dose of the photosensitizer and confined to the dark. After a drug-dependent period of equilibration during which most of the photosensitizer accumulates preferentially in the tumour tissue, the patient is anaesthetized, and a dose of light is administered using an appropriate light delivery technique, such as an optic fibre from a laser source. Tumour cell destruction begins almost immediately and a period of time is allowed for the photosensitizer and its metabolites to be eliminated from the body, before the patient is allowed back into the light (Okunaka et al 1995).

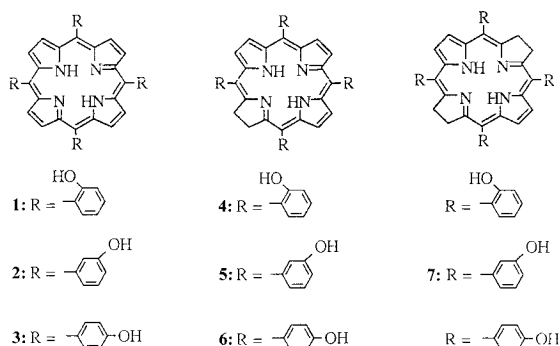


**Figure 1** The structures of the porphyrins 1–7.

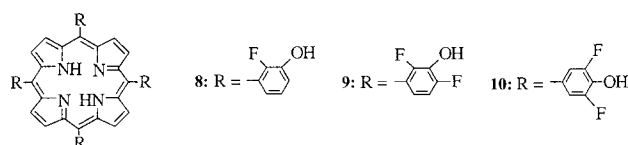


**Figure 2** The structures of the fluorinated analogues 8, 9, and 10 of the isomeric tetrahydroxyphenylporphyrins 1, 2, and 3 in which the fluorine substituents are *ortho* to the hydroxy groups.

In one of the earliest appearances of the tetrahydroxyphenylporphyrins 1, 2, and 3 (Figure 1) as a class of porphyrins with potential for use as photodynamic therapeutic photosensitizers, Berenbaum et al (1986) reported a comparison of these three isomeric *meso*-tetra(hydroxyphenyl)porphyrins, with HpD and Photofrin II in their ability to photosensitize tumours in mice. Later Bonnet et al (1989) reported the synthesis and bioassays of the three 2,3-dihydroporphyrins 4, 5, and 6 (Figure 1) respectively derived from the *meso*-tetra(hydroxyphenyl)porphyrins, 1, 2, and 3, and the 2,3,12,13-tetrahydroporphyrin 7 (Figure 1), derived from the *meso*-tetra(hydroxyphenyl)porphyrin 2. The synthesis, in-vitro bioassays, photophysical properties, and clinical applications of this class of porphyrin compounds in photodynamic therapy, which appeared subsequently in several reports, have demonstrated the widening application and the recognition of the effectiveness of this series of photosensitizers in photodynamic therapy (Bonnet et al 1988; Bonnet & Djelal 1993; Moan & Berg 1994).

Recently, we reported a general method for the synthesis of fluorinated analogues 5,10,15,20-tetrakis(2-fluoro-3-hydroxyphenyl)porphyrin (8), 5,10,15,20-tetrakis(2,4-difluoro-3-hydroxyphenyl)porphyrin (9), and 5,10,15,20-tetrakis(3,5-difluoro-4-hydroxyphenyl)porphyrin (10) (Figure 2) of the isomeric tetrahydroxy-

phenylporphyrins 1, 2, and 3 in which the fluorine substituents are *ortho* to the hydroxy groups (Songca et al 1997). One aim for making these compounds was to improve their solubility in aqueous media, since these fluorine substitution patterns were expected to increase the acidity of the *ortho* hydroxy groups. Another aim was to use the fluorine substituents on these compounds as contrast agents to monitor tissue distribution of these compounds in tumour implanted mice using  $^{19}\text{F}$  NMR spectroscopy. Since this fluorine substitution pattern was expected to lower the hydrophobicities of the fluorinated compounds, we became interested in comparing the activities of the fluorinated compounds with that of the leading compound in the unfluorinated set, the chlorin 5, in-vitro. In this study we have reported the bioassays of these compounds using the colorimetric cell viability assay described by Mosmann (1983). We have described cancer and tissue distribution of the fluorinated porphyrins in mice, using  $^{19}\text{F}$  NMR spectroscopy.

### The Mosmann assay

The Mosmann assay quantitatively detects living, but not dead cells. The method is therefore used to measure cytotoxicity, and proliferation. The results of the assay are easily read on a scanning UV/vis spectrophotometer with a high degree of precision. The method is based on the cleavage of MTT, 3-(4,5-dimethylthiazol-2-yl)-2,5-diphenyl tetrazolium bromide (11, Figure 3). The tetrazolium ring is cleaved in active mitochondria by the action of dehydrogenase enzymes and so the reaction occurs in living cells only.

The method is useful in measuring anti-cell proliferation effects of photosensitizing drugs designed for photodynamic therapy in-vitro (Grebenova et al 1998; Fickweiler et al 1999; Tsai et al 1999). MTT in phosphate-buffered saline is added to flasks containing cells and photosensitizer in growth medium under sterile conditions, and these are incubated at 37°C until the development of colour ceases. This takes approximately 5 h. During this time viable cells react with MTT to produce the blue crystalline product 12 (Figure 3). Upon



**Figure 3** The reaction of MTT (11) to produce the blue crystalline product 12.

completion of the reaction, acidic isopropyl alcohol (isopropanol) is added to dissolve the dark blue crystals. The absorbance of the isopropyl alcohol solution of MTT is measured on a UV/vis spectrophotometer, using a test wavelength of 570 nm, a reference wavelength of 630 nm, and a calibration setting of 1.00. The colour intensity is normally measured within 1 h of adding the isopropyl alcohol, and is proportional to the concentration of viable cells in the growth medium. The survival fraction is based on the readings from a set of control flasks containing cells without treatment with photosensitizer (Mosmann 1983).

### <sup>19</sup>F NMR spectroscopy

In general, an important attraction of fluorinated analogues of porphyrin compounds for photodynamic therapy is the possibility of studying their localization in tissues by <sup>19</sup>F NMR spectroscopy, thus investigating tissue distribution in a non-invasive way. In addition to monitoring their tumour uptake and retention, <sup>19</sup>F NMR spectra of the fluorinated porphyrins can be measured in tumours and other organs of tumour implanted mice over a period of time, using an imaging nuclear magnetic resonance spectrometer, with a bore wide enough to fit a mouse (Wolf et al 2000).

## Materials and Methods

### Porphyrin synthesis

The compounds were prepared as reported by Songca et al (1997). The synthesis yielded at least 300 mg of each compound in spectroscopic purity (> 95%), with the porphyrin **10** showing a single spot on TLC, while the porphyrins **8** and **9** showed four atropisomeric spots. The porphyrin **2** and the chlorin **5** were prepared as previously described (Bonnett et al 1987, 1989). They were also obtained in spectroscopic purity as single spots on TLC. Stock solutions (20 mL) of 10 mg mL<sup>-1</sup> were prepared in dimethylsulfoxide and frozen at -5°C.

### Cell preparations

Chinese Hamster Ovarian (CHO) cell lines were grown in Hams F12 growth medium supplemented with 10% fetal calf serum and 1% penicillin, at 37°C in a 6% CO<sub>2</sub> atmosphere, under sterile conditions. The cells were suspended by treating with EDTA followed with trypsin, centrifugation and re-suspension in the growth medium.

The cells were counted on a Gouy apparatus for re-growth in the incubation flasks (Mosmann 1983).

### Bioassay

A solution of MTT in phosphate-buffered saline (5 mg mL<sup>-1</sup>) was added to incubation flasks each containing 400 cells and photosensitizer in growth medium under sterile conditions. The flasks were incubated at 37°C for 4 h, after which no further colour development was observed. Acidic isopropyl alcohol was added to dissolve the blue crystals. The absorbance was measured on a Perkin Elmer UV/vis spectrophotometer, using a test wavelength of 570 nm, a reference wavelength of 630 nm, and a calibration setting of 1.00. The percentage fraction of surviving cells was calculated for each flask, based on a series of control flasks containing 400 cells in growth medium, but without photosensitizer. To evaluate the combined effect of the photosensitizer and radiation, the flasks were irradiated with 150 J cm<sup>2</sup> from an Oxford Lasers laser dye light source with a bandwidth of 630–660 nm, just before incubation, and then the same procedure was followed as above (Mosmann 1983). These measurements were performed in triplicate with good reproducibility (1.5% < standard deviation < 5.9%), and the mean values were reported.

### <sup>19</sup>F NMR spectroscopy

Three BALB/c mice, each bearing a tumour that had been grown in the right thigh from subcutaneously implanted PC6 plasma cell tumours, were each injected with one of the three different porphyrins. Mouse 1 and mouse 2 were respectively injected with 0.5 mL 2.43 × 10<sup>-2</sup> M solutions of **9** and **10** in 40% aqueous ethanol, while mouse 3 was injected with 0.5 mL of a 8.03 × 10<sup>-3</sup> M solution of **8**. The injections were carried out at 0900 h at room temperature. At 1100 h the mice were anaesthetized, carefully placed on the imaging probe and inserted into the magnet. All spectra and images were recorded on a CISCO-200 imaging spectrometer, equipped with a 30-cm horizontal bore superconducting magnet running at 4.7T. To ascertain that the anatomic area of each animal under observation was indeed the tumour area, several <sup>1</sup>H NMR images of the right thigh were taken, slicing from the region of the spinal cord working outwards through the tumour, towards the coil. The tumours were clearly observed (see Figure 4A–D). <sup>19</sup>F NMR spectra of the tumours and various organs of the mice were measured, by simply placing the coil over the organ under observation, carefully placing the mouse in the probe, inserting into

the magnet and measuring the spectrum. Each spectrum was recorded from 512 45° pulses and a total accumulation time of 8.5 min.

### Results and Discussion

Although all the compounds 1–7 have been reported to give substantial tumour photo-necrosis, in this study the chlorins 4–6 were found to be more active than the porphyrins 1–3, and the bacteriochlorin 7 was found to be more active than the chlorins 4–6 (Berenbaum et al

1986; Bonnett et al 1989). Clearly therefore, in this set of compounds, activity is influenced by the extent of hydrogenation of the photosensitizer. Solutions of chlorins and bacteriochlorins are relatively unstable, easily reverting to the porphyrins under weakly oxidizing conditions, such as exposure to atmospheric oxygen. However, chlorins are more stable than bacteriochlorins, although they too easily revert to the corresponding porphyrins. Consequently, detailed studies were conducted on the properties and applications of the chlorins, from which the chlorin 5 emerged as the most suitable compound in the set (Bonnet et al 1987, 1988, 1989;

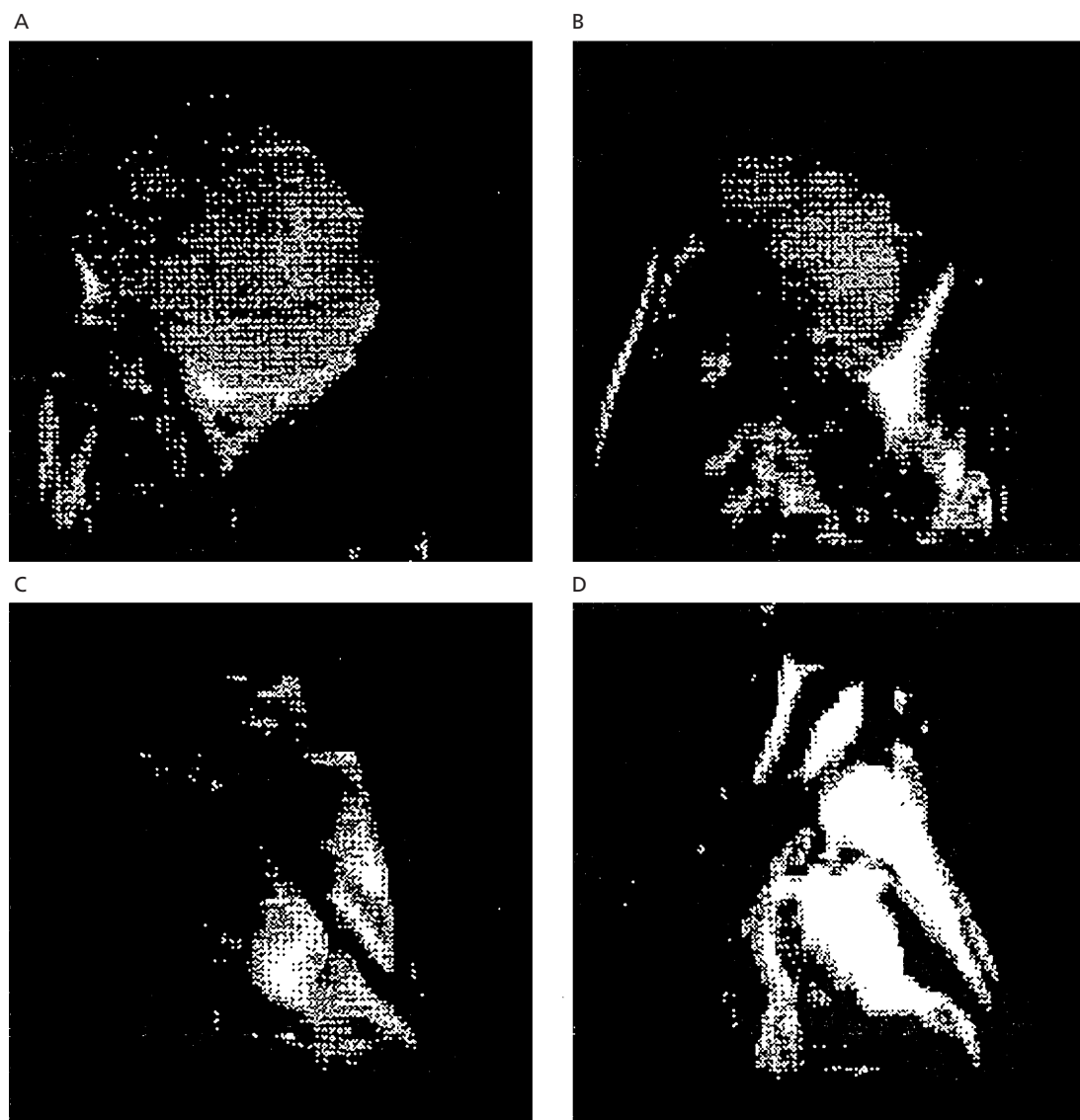


**Figure 4**  $^1\text{H}$  NMR images of the tumour of mouse 1. The images A–D were taken at depths of 5, 6, 7 and 8 mm, respectively. The tumour is visible as white patches within the black background. Scale is approximately 4:1.

Bonnet & Djelal 1993; Moan & Berg 1994). This compound is currently approved in the UK as a photodynamic therapy photosensitizer for head and neck cancers, and is undergoing various stages of clinical trials for a variety of other indications (Kessel 1998).

### The Mossman assay

The results of the Mossman assay on the fluorinated porphyrins 8–10 suggested that the activity of these compounds *in-vitro* approached that of the chlorin 5. Comparison of the effect of the chlorin 5 with that of the fluorinated porphyrin 8 on the survival of cells in the dark and after irradiation is shown in Figure 5A. These

results suggested that the toxicity of the porphyrin 8 in the dark was roughly 10–20% more than that of the chlorin 5, and that the toxicities of the two compounds after irradiation were fairly comparable within the photosensitizer concentration range of 0–1.0 g mL<sup>-1</sup>. Comparison of the effect of the chlorin 5 to that of the fluorinated porphyrin 9 (Figure 5B) suggested that the toxicity of the porphyrin 9 after irradiation compared favourably with that of the chlorin 5, within the photosensitizer concentration range of 0–1.0 g mL<sup>-1</sup>. Within this concentration range, the porphyrin 9 was almost as toxic as the chlorin 5 in the dark. Figure 5C shows that the fluorinated porphyrin 10 showed the highest toxicity in the dark. After irradiation this porphyrin was still roughly 10% less toxic than the chlorin 5.

These results suggested that the fluorinated set of porphyrins in which the fluorine substituents were adjacent to the hydroxy groups warrant further investigation as potentially potent photosensitizers for photodynamic therapy, since their toxicity in the dark was not so prohibitive, while their phototoxicities approached that of the chlorin 5. Based on the trend observed with the biological activities of the porphyrins 1–3, their 2,3-dihydro and their 2,3,12,13-tetrahydro derivatives 4–7, the 2,3-dihydro and 2,3,12,13-tetrahydro derivatives of the fluorinated porphyrins are expected to show even better activity than that of the unfluorinated counterparts.

Recently, we showed that the effect of the fluorine substitution pattern in which the fluorine substituents were adjacent to the hydroxy groups on the hydrophobicity of these compounds was to lower their partition coefficients between 2-octanol and phosphate-buffered saline, from approximately  $6.0 \times 10^4$  to approximately  $3.5 \times 10^4$  (Songca & Mbatha 2000). Although this is not a large enhancement of hydrophilicity, it is expected to be sufficient to enhance the plasma mobility of these photosensitizers, while retaining their trans-membrane mobility and intracellular localization, due to the overall relative hydrophobicity of their macrocyclic nuclei. It is expected therefore that the uptake and retention of these fluorinated compounds by, and consequently their preferential localization in, cancer tissue will be enhanced.

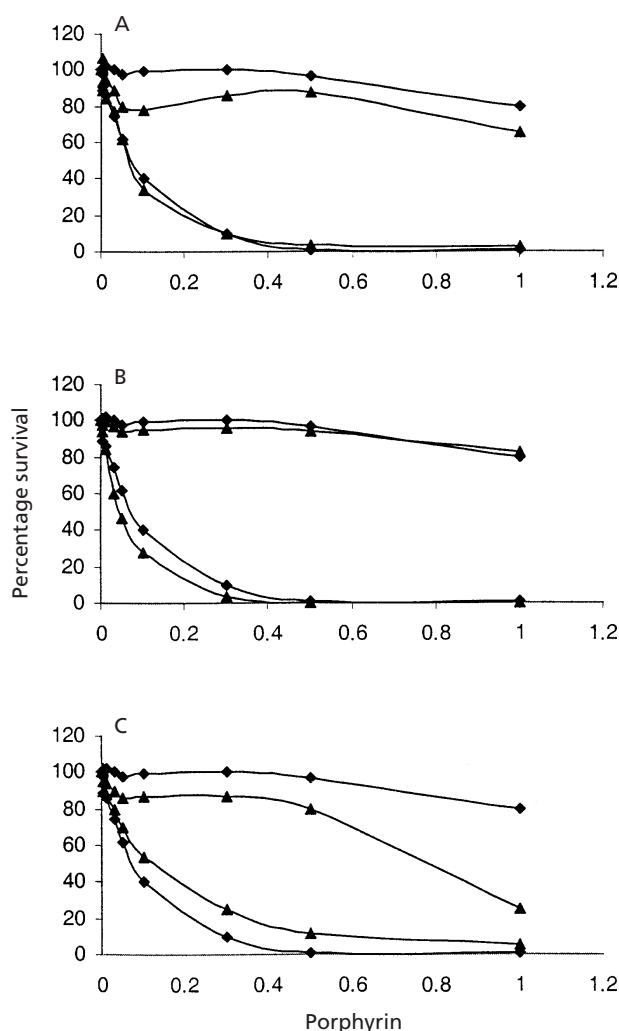


**Figure 5** Percentage survival fractions of CHO cells treated with porphyrins in the dark (top curves) and after irradiation (bottom curves). (A) 5 (◆) and 8 (▲). (B) 5 (◆) and 9 (▲). (C) 5 (◆) and 10 (▲).

### <sup>19</sup>F NMR spectroscopy

The uptake and retention of the fluorinated photosensitizers and their tumour localization were investigated using <sup>19</sup>F NMR spectroscopy. The *in-vivo* <sup>19</sup>F NMR spectra of 8 (Figure 6A) indicated that good

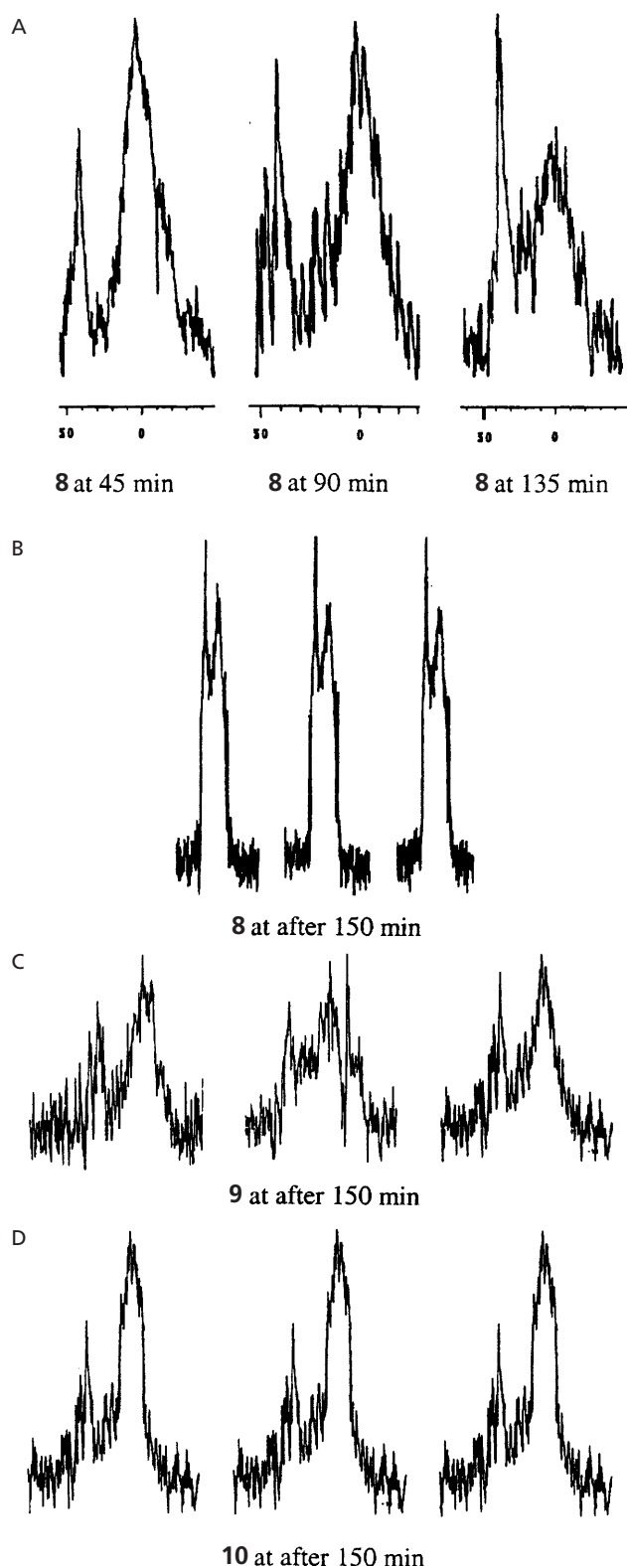


**Figure 6**  $^{19}\text{F}$  NMR signals of the tumours of the mice at various times after injection with the fluorinated porphyrins **8**, **9**, and **10**.

**Table 1** Signal-to-noise ratios of the signals obtained from the implanted tumours and from various organs of the mice.

Porphyrin	<b>8</b>	<b>9</b>	<b>10</b>
Implanted tumour	18	5	10
Abdomen	0.5	0.6	1.5
Thoracic cavity	0.5	0.9	1.3
Brain	2.0	1.6	1.8

signal detectability (signal-to-noise ratio 5–18) could be obtained on injecting approximately  $5 \times 10^{-6}$  mol porphyrin into the mouse. The  $^{19}\text{F}$  NMR spectrum of the tumour of mouse 1 showed two signals, one sharp signal approximately 40 ppm downfield of a broad signal (Figure 6A). Monitoring this signal showed that it varied significantly with time (Figure 6A). The intensity of the downfield signal was increasing in relation to the upfield signal, for approximately 135 min, after which time both signals remained relatively constant for the rest of the experiments (Figure 6A–B). This variation was observed with all the mice and was attributed to the pharmacokinetics of the photosensitizer within the tumour. The general presence of two signals was interpreted to indicate that the porphyrin was being detected in two chemical environments, which were sufficiently different to give different signals. One possibility was that one signal arose from the porphyrin in the blood stream and the other one from the localized porphyrin. The  $^{19}\text{F}$  NMR spectra obtained from selected organs of the animals were qualitatively similar to those observed from the tumours.

As a semi-quantitative measure of the tissue distribution of the fluorinated porphyrins, the  $^{19}\text{F}$  NMR signal-to-noise ratios of the signals measured 150 min after injection in the various organs of the mice are given in Table 1. Table 1 shows that signal-to-noise ratios of the signals obtained from the organs of the mice where no cancer was implanted were all in the range 0.5–2. The signal-to-noise ratios of the signals from the implanted cancers were in the range 5–18. This data suggested that the ratio of the concentration of porphyrin **8** in cancer tissue to that in normal tissue may be estimated as 9:1. Similarly for the porphyrins **9** and **10** this ratio was approximately 3:1 and 5:1, respectively. This study showed that the uptake and retention of these fluorine containing porphyrins could be monitored in-vivo by low resolution  $^{19}\text{F}$  NMR spectroscopy within reasonable accumulation times ( $< 30$  min) with doses of approximately  $5 \times 10^{-6}$  mol porphyrin per animal. These measurements could be used to estimate the ratio of porphyrin in cancer tissue to that in normal

tissue, a good measure of tumour selectivity of the porphyrin sensitizers.

## References

- Berenbaum, M. C., Akande, S. L., Bonnett, R., Kaur, H., Ioanou, S., White, R. D., Winfield, U.-J. (1986) *meso*-Tetra(hydroxyphenyl)porphyrins, a new class of potent tumour photosensitizers with favourable selectivity. *Br. J. Cancer* **54**: 717–725
- Bonnet, R., Djelal, B. (1993) *m*-THPC. *Photodynamics* **6**: 2–4
- Bonnett, R., Ioannou, S., White, R. D., Winfield, U.-J., Berenbaum, M. C. (1987) *Photobiochem. Photobiophys.* (Suppl.) 45–56
- Bonnett, R., McGarvey, D. J., Harriman, A., Land, E. J., Truscott, T. G., Winfield, U.-J. (1988) Photophysical properties of *meso*-tetraphenylporphyrin and some *meso*-tetra(hydroxyphenyl)porphyrins. *Photochem. Photobiol.* **48**: 271–276
- Bonnett, R., White, R. D., Winfield, U.-J., Berenbaum, M. C. (1989) Hydroporphyrins of the *meso*-tetra(hydroxyphenyl)porphyrin series as tumour photosensitizers. *Biochem. J.* **261**: 277–280
- Fickweiler, S., Abels, C., Karrer, S., Baumler, W., Landthaler, M., Hofstadter, F., Szeimies, R. M. (1999) Photosensitization of human skin cell lines by ATMPn (9-acetoxy-2,7,12,17-tetrakis-(beta-methoxyethyl)-porphycene) in-vitro: mechanism of action. *J. Photochem. Photobiol. B* **48**: 27–35
- Grebenova, D., Cajthamlova, H., Bartosova, J., Marinov, J., Klamova, H., Fuchs, O., Hrkal, Z. (1998) Selective destruction of leukaemic cells by photo-activation of 5-aminolaevulinic acid-induced protoporphyrin-IX. *J. Photochem. Photobiol. B* **47**: 74–81
- Kessel, D. (1998) PDT: expanding the database, an update on new drugs and mechanism of phototoxicity. *Int. Photodynamics* **1**: 2–4
- Moan, J., Berg, K. (1994) Evaluation of a new photosensitizer, *meso*-tetra-hydroxyphenyl-chlorin, for use in photodynamic therapy: a comparison of its photobiological properties with those of two other photosensitizers. *Int. J. Cancer* **57**: 883–888
- McRobert, A. J., Bown, S. G., Phillips, D. (1989) What are the ideal photoproperties for a sensitizer? In: Bock, G., Harnett, S. (eds) Ciba Foundation Symposium 146: *Photosensitising compounds: their chemistry and biological use*. John Wiley & Sons, Chichester, UK, pp 4–12
- Mosmann, T. (1983) Rapid colorimetric assay for cellular growth and survival: application to proliferation and cytotoxicity assays. *J. Immunol. Methods* **65**: 55–63
- Neely, W. C., Martin, J. M., Barker, S. A. (1988) Products and relative reaction rates of the oxidation of tocopherols with singlet molecular oxygen. *Photochem. Photobiol.* **48**: 423–428
- Okunaka, T., Kato, H., Konaka, C. (1995) A clinical trial of photodynamic therapy for early stage lung cancer. *Int. Photodynamics* **1**: 4–6
- Songca, S. P., Mbatha, B. (2000) Solubilisation of *meso*-tetraphenylporphyrin photosensitizers. *J. Pharm. Pharmacol.* **52**: 1–8
- Songca, S. P., Bonnett, R., Maes, C. (1997) A convenient route to new fluorinated photodynamic therapeutic photosensitizers based on *meso*-tetra(hydroxyphenyl) porphyrins. *S. Afr. J. Chem.* **50**: 40–47
- Tsai, J. C., Hsiao, Y. Y., Teng, L. J., Chen, C. T., Kao, M. C. (1999) Comparative study on the ALA photodynamic effects of human glioma and meningioma cells. *Lasers Surg. Med.* **24**: 296–305
- Wolf, W., Presant, C. A., Waluch, V. (2000) <sup>19</sup>F-MRS studies of fluorinated drugs in humans. *Adv. Drug Deliv. Rev.* **15**: 55–74